Vibrational Echo Studies of Protein Dynamics

C. W. Rella,[1] Alfred Kwok,[2] Kirk Rector,[2] Jeffrey R. Hill,[3] H. A. Schwettman,[1] Dana D. Dlott,[3,*] and M. D. Fayer [2,*]

[1]*Stanford Free Electron Laser Center, Hansen Experimental Physics Laboratory, Stanford University, Stanford, California 94305-4085*

[2]*Department of Chemistry, Stanford University, Stanford, California 94305*

[3]*School of Chemical Sciences, University of Illinois at Urbana-Champaign, Urbana, Illinois 61801*

(Received 10 April 1996)

The first picosecond infrared vibrational echo experiments on a protein, myoglobin-CO, are described. The experiments were performed at temperatures ranging from 60 to 300 K with a midinfrared free electron laser tuned to 1945 cm^{-1}. Below ~185 K, the pure dephasing, T_2^*, displays a power law temperature dependence, $T^{1.3}$. This behavior is reminiscent of that associated with the properties of low temperature glasses (<5 K) but is observed here at much higher temperatures. Above the solvent glass transition temperature, T_2^* is exponentially activated. [S0031-9007(96)00882-4]

PACS numbers: 87.15.He

We present the first vibrational echo experiments performed on a protein. These experiments provide a new method for examining protein dynamics. The vibrational echo [1] is the vibrational analog of the spin echo of NMR [2] and the photon echo of visible and UV spectroscopy [3]. The advent of spin echo in 1950 ushered in a new dimension in magnetic resonance spectroscopy [2]. Like the spin echo, the vibrational echo is expanding the scope of infrared vibrational spectroscopy. The vibrational echo experiment gains its importance because it permits the homogeneous vibrational line shape, which is the result of dynamics, to be extracted from an inhomogeneously broadened vibrational spectrum.

The experiments were performed on the vibrational stretching mode of carbon monoxide (CO) bound to the active site of myoglobin (Mb). By combining vibrational echo measurements with vibrational pump-probe lifetime measurements, the pure dephasing time T_2^* is determined [1]. Previous optical coherence experiments performed on proteins examined the dephasing of electronic transitions at a few degrees K [4]. In contrast, the vibrational echo experiments make it possible to use optical coherence methods to study protein dynamics at physiologically relevant temperatures.

Myoglobin is used in the storage and transport of dioxygen (O_2) in muscle tissue [5]. It consists of a prosthetic group called protoheme [Fe(II)protoporphyrin IX] embedded in a protein. The protein modifies the chemical reactivity of the Fe binding site, allowing Mb to function properly in a biological setting [5].

When bound at the Mb active site, the CO frequency is strongly redshifted from its gas phase value and separated into four distinct bands, labeled A_0–A_3 in order of decreasing stretch frequency [6]. In principle, information about vibrational dynamics can be obtained from the Fourier transform of the linear absorption spectra. Finite lifetime and vibrational dephasing due to time dependent perturbations of the transition frequency lead to homogeneous broadening. In a disordered condensed matter system such as Mb-CO, however, even a well resolved vibrational spectrum does not provide information on dynamics. The spectral line is inhomogeneously broadened by the distribution of protein conformations that result in a distribution of protein-CO interactions. The IR absorption spectrum is a convolution of the various dynamic and static contributions to the observed line shape. Inhomogeneous broadening cannot be eliminated with linear spectroscopy [7].

The infrared vibrational echo experiment is a time domain nonlinear method which can extract the homogeneous vibrational line shape from inhomogeneously broadened lines [1,8]. In 1964, the magnetic resonance spin echo method was extended to the visible optical regime as the photon echo [3]. Recently, vibrational echoes have been used to examine vibrational dynamics in liquids and glasses [1,8].

In the vibrational echo experiment, the sample is irradiated by an intense pulse which coherently drives the ensemble of CO oscillators. These oscillators lose phase coherence due to homogeneous and inhomogeneous broadening. A second intense pulse, incident at time τ after the first, causes a partial rephasing. The rephasing generates a macroscopic polarization at time 2τ, and, thus, the emission of a third pulse of light, the echo. The echo signal, which is emitted in a unique direction, is measured as a function of delay time τ.

An exponential vibrational echo decay corresponds to a Lorentzian line shape with a width, Γ, given by

$$\Gamma = \frac{1}{\pi T_2} = \frac{1}{\pi T_2^*} + \frac{1}{2\pi T_1}, \tag{1}$$

where T_2 is the homogeneous dephasing time determined from the echo decay constant, and T_1 is the vibrational lifetime determined from pump-probe experiments. Measurements of T_2 and T_1 permit the determination of T_2^*, the pure dephasing time. The vibrational echo decay signal $S(t)$ is given by

$$S(t) = S_0 e^{-4\tau/T_2}. \tag{2}$$

 0031-9007/96/77(8)/1648(4)$10.00

The experiments were conducted using ps infrared pulses from the Stanford Free Electron Laser (FEL). The FEL pulse train consists of a macropulse of about 3 ms length repeating at 10 Hz, within which is contained a series of micropulses repeating at 11.8 MHz. Each micropulse has an energy of $\sim 1\ \mu$J and is nearly a transform-limited Gaussian 1.7 ps in duration. The laser was tuned to the A_1 band at 1945 cm^{-1}, and was actively stabilized to within $2 \times 10^{-2}\%$ of the center frequency. Both the autocorrelation and the spectrum were monitored continuously during the experiments.

The vibrational echo and pump-probe experiments were performed using essentially the same experimental apparatus illustrated in Fig. 1. Micropulses were selected from the macropulse at a 50 kHz repetition rate using a fast germanium acousto-optic modulator (AOM). A fraction of the beam (50% for the echo, 10% for the pump probe) was picked off using a beam splitter and sent directly to the sample. The remainder of the beam passed through a second AOM, which chopped the beam to enable the detection electronics to suppress noise due to scattered light and intensity fluctuations. This beam was sent down a computer controlled optical delay line and then to the sample. The two infrared beams were focused to a diameter of 100 μm on the myoglobin sample. Echo pulse and pump pulse energies of 150–300 nJ were typical, with probe pulse energy $\sim$20 nJ.

The sample was a 15 m*M* solution of wild type horse heart myoglobin in buffered 95% glycerol/5% H_2O saturated with CO. The sample had a path length of 125 μm and was cooled with a helium flow cryostat. The Mb-CO absorption is a peak with an absorbance of 0.3 on a very broad background of absorbance $\cong$1. Despite this, it is possible to obtain high quality vibrational echo data because the nonlinear nature of the method rejects contributions from the background, which arises from a large number of weak transitions.

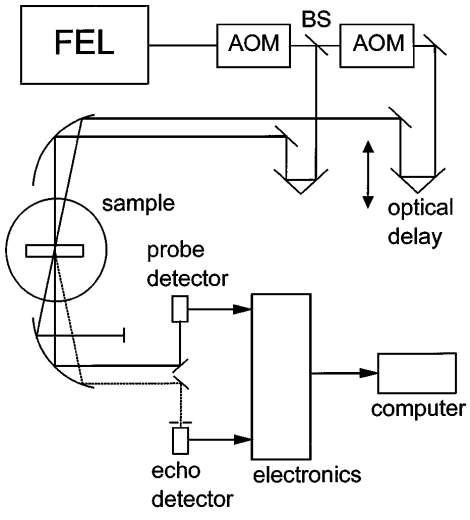

FIG. 1. Schematic of the experimental apparatus used for both the vibrational echo and pump-probe experiments. The only significant differences between the two setups are in the timing of the acousto-optic modulators (AOMs) and in the choice of beam splitter (BS): 50% reflectance for the echo and 10% reflectance for the pump probe.

Vibrational echo measurements were taken from 60 to 300 K. Several decay curves were taken at each temperature. Figure 2 displays a typical echo decay curve taken at 80 K; the inset is a semilogarithmic plot of this same data. The signal-to-noise ratio is quite good in spite of the large background absorption of the sample. The solid line through the data in the inset is the result of an exponential fit. The echo decays at all temperatures are fit well by a single exponential except for the 300 K point for which the fit included convolution with the Gaussian instrument response. The homogeneous line shape is Lorentzian at all temperatures.

The vibrational dephasing arises from fluctuations in the protein structure, not from the surrounding solvent. Linear vibrational spectroscopy [6,9] shows that the spectrum is extremely sensitive to structural changes of the protein, e.g., the position of the distal histidine, and is insensitive to changing the solvent. Because of the strong coupling between the protein structure and the CO frequency, protein fluctuations produce significant variations in the CO frequency and are the dominant source of vibrational dephasing. A variety of other factors, which will be discussed in a subsequent publication [10], give additional support to the concept that protein fluctuations are responsible for pure dephasing.

The mechanism that couples the protein to the CO, described in detail elsewhere [10], involves fluctuations in the back donation of heme π electron density into the CO π^* antibonding molecular orbital. Static changes in back donation are responsible for shifts in the CO vibrational frequency, and these are caused by changes in protein structure [11]. Thus, the pure dephasing can be caused by dynamic changes in protein structure inducing

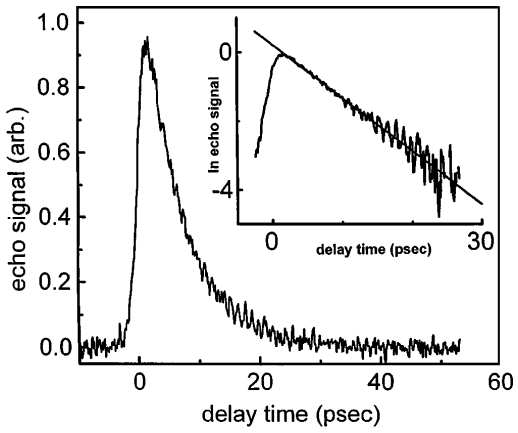

FIG. 2. Vibrational echo data on Mb-CO in glycerol/water at 80 K. The inset displays the same data on a semilogarithmic plot along with the fit to the data, which shows that the echo decay is exponential over a wide dynamic range.

fluctuations in back donation, and, therefore, variations in the vibrational frequency.

At 80 K, the echo data yield $T_2 = 26.5 \pm 0.6$ ps, corresponding to a homogeneous linewidth of 0.40 cm^{-1}. The width of the absorption spectrum at 80 K is 12 cm^{-1}. Therefore, the line is massively inhomogeneously broadened, with the two widths differing by a factor of 30. At room temperature, the homogeneous linewidth is 2.7 ± 0.5 cm^{-1}, which is still approximately 5 times narrower than the 13 cm^{-1} width of the room temperature absorption spectrum. The observation of inhomogeneous broadening at room temperature allows us to conclude that on the echo time scale the protein exists in many different conformational substates, each characterized by different transition frequency of the CO stretch.

Pump-probe lifetime measurements were made over the same range of temperatures. The temperature dependent T_1 and T_2 data, as well as the pure dephasing times, T_2^*, obtained using Eq. (1), are displayed in Fig. 3. T_1 and T_2 could be determined from the data within $\pm 3\%$ error. The error in the derived quantity T_2^* is approximately $\pm 5\%$.

Figure 4 displays the pure dephasing rate, $1/T_2^*$, on a logarithimic plot. The temperature dependence of the pure dephasing rate is less steep at low temperatures. There is a break in the temperature dependence at $\sim$185 K, which is within the range of temperatures associated with the glass transition temperature of the glycerol/water solvent. Below this transition, the data fall on a straight line, indicating power law behavior of the form aT^α, where $\alpha = 1.3 \pm 0.05$. This fit is indicated by the dashed line in Fig. 4.

The $T^{1.3}$ dependence is reminiscent of the temperature dependence that has been observed for the pure dephasing rate of electronic transitions of molecules in low temperature glasses [12]. Several experiments, including ligand recombination studies [13] and pressure relaxation experiments [14], suggest that protein behavior is similar to that of glasses in many ways. Furthermore, protein simulations demonstrate the existence of many conformations that involve only small structural changes [15]. It is, therefore, reasonable to analyze the protein dephasing data using the techniques developed for the study of glasses.

Although there have been several theoretical treatments of glasses, the most successful by far has been the tunneling two-level system (TLS) model [16]. The TLS model postulates that some atoms or molecules (or groups of atoms or molecules) can reside in either of two minima of the local potential surface. Each side of the double well potential represents a distinct local configuration of the glass. The bulk glass material contains an ensemble of these two-level systems characterized by a broad distribution of energy differences and tunneling parameters. Transitions occur via tunneling through the potential barriers, or, at sufficiently high temperatures, by activation over these barriers. Thus, the complex potential surface is modeled as a collection of double well potentials.

The low temperature pure dephasing linewidths can be calculated using the TLS uncorrelated sudden jump model [12,17]. It is found that the temperature dependence of the homogeneous dephasing rate is a power law, T^α, where α is determined by the probability distribution, $P(E)$, for the TLS energy difference, E. If $P(E)$ equals a constant, i.e., there is an equal probability of all TLS splittings, and the distribution of tunneling parameters is also flat, then $\alpha = 1$. In general, for $P(E) \propto E^\mu$, $\alpha = 1 + \mu$.

The $T^{1.3}$ temperature dependence observed in Mb-CO can be understood in terms of a tunneling protein two-level system (PTLS) model. A protein is a nonequilibrium system with many possible conformations. Conformational changes can be viewed as occurring via motion on a multidimensional potential surface. The PTLS model represents this complex potential surface as a

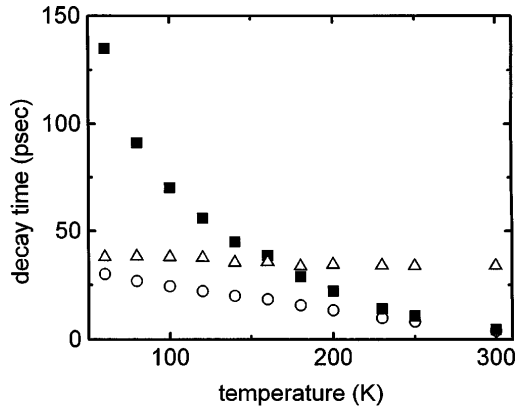

FIG. 3. Plot of twice the measured excited state lifetime $2T_1(\Delta)$, the total dephasing time $T_2(\bigcirc)$, and the pure dephasing $T_2^*(\blacksquare)$, derived from the first two quantities using Eq. (1). At high temperatures, the total dephasing, T_2, is dominated by pure dephasing; at low temperatures, the total dephasing arises mainly from T_1.

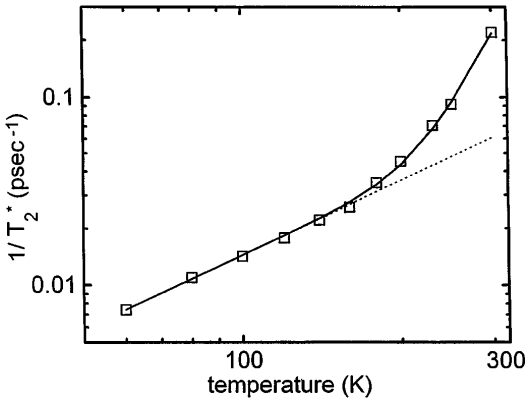

FIG. 4. Plot of the natural logarithm of $1/T_2^*$ vs the natural logarithm of temperature. Below the solvent's glass transition temperature ($\sim$185 K), the data follow a power law, $T^{1.3}$ dependence, indicated by the dashed line in the figure. Above the glass transition, the data are exponentially activated with $\Delta E \approx 1000$ cm^{-1}.

collection of double well potentials, each side representing a different protein conformation. Each protein molecule contains many PTLS, which are associated with the possible conformational changes that can occur. The wells have a variety of energy differences, barrier heights, and tunneling parameters.

In the context of the uncorrelated sudden jump model, the observed $T^{1.3}$ temperature dependence implies that $P(E) = E^{0.3}$. This is a very flat distribution of energies. The PTLS model of the Mb protein indicates that the protein has an energy landscape on which the distribution of energy differences between conformations is broad and almost flat. The energies involved are much greater than those invoked to explain dynamics in low temperature glasses. Experiments on proteins at low temperature (2 K) indicate that proteins also have very low energy potential barriers [4]. The results presented here suggest that there are also higher barriers in Mb that play an important role at temperatures on the order of 100 K. Tunneling through barriers in the 100 K range is in contrast to glasses in which dynamics at such elevated temperatures are dominated by phonons or activation over low energy barriers [12,16].

The PTLS model is capable of explaining the observed vibrational dephasing temperature dependence below the solvent glass transition temperature. It builds on the extensive history of considering proteins in terms of concepts that have been applied to glasses [14]. A theoretical investigation is currently in progress to determine if a less restrictive model of protein fluctuations can account for the observed power law temperature dependence.

Above the solvent glass transition, the Mb-CO dephasing dynamics exhibit a clear deviation from the low temperature power law behavior. This change can likely be attributed to the softening of the boundary condition placed on protein motions by the solvent. Barriers to conformational change that were insurmountable with the rigid glassy boundary condition will become lower when the solvent becomes a liquid permitting conformational changes via activation over barriers. We can model this process by fitting the dephasing rate with an activation term, $be^{-\Delta E/kT}$, where ΔE is the barrier height. Thus,

$$\frac{1}{T_2^*} = aT^{\alpha} + be^{-\Delta E/kT}. \quad (3)$$

The solid line in Fig. 4 is a result of the fit by this equation, with $\Delta E = 1250 \pm 200\ \mathrm{cm}^{-1}$. It is possible that the tunneling term is less significant above the transition temperature. This would reduce the ΔE. The net result is that the high temperature data are fit by an activation energy on the order of $1000\ \mathrm{cm}^{-1}$.

We have presented the first vibrational echo experiments performed on a protein. Vibrational echo experiments are a new method for examining protein dynamics and have already yielded some intriguing insights into how protein dynamics are transmitted to the active site of myoglobin. Future experiments will examine mutant Mb and other heme-CO proteins to investigate how specific structural features influence protein dynamics at the active site.

This research was supported by the Medical Free Electron Laser Program, through the Office of Naval Research, Contract No. N00014-94-1-1024 (C.W.R., M.D.F., A.K., H.A.S.). Additional support was provided by the Office of Naval Research, Biology Division, Contract No. N00014-95-1-0259, and the National Science Foundation, Division of Materials Research Grant No. DMR94-04806 (D.D.D., J.R.H.), and the National Science Foundation, Division of Materials Research, Grant No. DMR93-22504 (K.R., M.D.F.).

*To whom correspondence should be addressed.

[1] D. Zimdars, A. Tokmakoff, S. Chen, S. R. Greenfield, M. D. Fayer, T. I. Smith, and H. A. Schwettman, Phys. Rev. Lett. **70**, 2718 (1993); A. Tokmakoff, D. Zimdars, R. S. Urdahl, R. S. Francis, A. S. Kwok, and M. D. Fayer, J. Phys. Chem. **99**, 13 310 (1995).

[2] E. L. Hahn, Phys. Rev. **80**, 580 (1950).

[3] N. A. Kurnit, I. D. Abella, and S. R. Hartmann, Phys. Rev. Lett. **13**, 567 (1964).

[4] D. T. Leeson and D. A. Wiersma, Phys. Rev. Lett. **74**, 2138 (1995).

[5] E. B. M. Antonini, *Hemoglobin and Myoglobin in Their Reactions with Ligands* (North Holland, Amsterdam, 1971).

[6] A. Ansari *et al.,* Biophys. Chem. **26**, 337 (1987).

[7] R. F. Loring and S. Mukamel, J. Chem. Phys. **83**, 2116 (1985).

[8] A. Tokmakoff and M. D. Fayer, J. Chem. Phys. **102**, 2810 (1995).

[9] Dmitri Ivanov, J. Timothy Sage, Markus Keim, Jay R. Powell, Sanford A. Asher, and Paul M. Champion, J. Am. Chem. Soc. **116**, 4139 (1994).

[10] C. W. Rella, Kirk Rector, Alfred Kwok, Jeffrey R. Hill, H. A. Schwettman, Dana D. Dlott, and M. D. Fayer, J. Phys. Chem. (to be published).

[11] X. Y. Li and T. G. Spiro, J. Am. Chem. Soc. **110**, 6024 (1988). K. D. Park, K. Guo, F. Adebodun, M. L. Chiu, S. G. Sligar, and E. Oldfield, Biochemistry **30**, 2333 (1991); E. Oldfield, K. Guo, J. D. Augspurger, and C. E. Dykstra, J. Am. Chem. Soc. **113**, 7537 (1991).

[12] M. Berg, C. A. Walsh, L. R. Narasimhan, Karl A. Littau, and M. D. Fayer, J. Chem. Phys. **88**, 1564 (1988); L. R. Narasimhan, K. A. Littau, Dee William Pack, Y. S. Bai, A. Elschner, and M. D. Fayer, Chem. Rev. **90**, 439 (1990), and references therein.

[13] R. H. Austin, K. Beeson, L. Eisenstein, H. Frauenfelder, I. C. Gunsalus, and V. P. Marshall, Phys. Rev. Lett. **32**, 403 (1974).

[14] I. E. T. Iben *et al.,* Phys. Rev. Lett. **62**, 1916 (1989); H. Frauenfelder *et al.,* J. Phys. Chem. **94**, 1024 (1990).

[15] R. Elber and M. Karplus, Science **235**, 318 (1987).

[16] P. W. Anderson, B. I. Halperin, and C. M. Varma, Philos. Mag. **25**, 1 (1972). W. A. Phillips, J. Low Temp. Phys. **7**, 351 (1972).

[17] Y. S. Bai and M. D. Fayer, Phys. Rev. B **39**, 11 066 (1989).